Strain-induced magneto-optical anisotropy in epitaxial hcp Co films

J. A. Arregi,* J. B. González-Díaz, O. Idigoras, and A. Berger
CIC nanoGUNE Consolider, Tolosa Hiribidea 76, E-20018 Donostia–San Sebastián, Spain
(Received 14 February 2014; revised manuscript received 9 September 2015; published 3 November 2015)

We investigate the existence and origin of magneto-optical anisotropy in epitaxial hcp Co films. Our results show that a significant magneto-optical anisotropy exists in our samples and, more importantly, they reveal that its amplitude is directly correlated with epitaxial strain. We find a linear coefficient of 16.8% magneto-optical anisotropy per every 1% epitaxial strain, which is in stark contrast to an isotropic magneto-optical coupling factor Q, a very frequent and common assumption in magneto-optics of metallic thin films and multilayers. In addition, the Co films exhibit a similar strain-induced increase of the magnetocrystalline anisotropy energy, evidencing the fact that both magneto-optical anisotropy and magnetocrystalline anisotropy are dependent on the modification of the spin-orbit coupling introduced by anisotropic lattice distortions.

DOI: 10.1103/PhysRevB.92.184405 PACS number(s): 78.20.Ls, 68.60.Bs, 75.60.Jk

I. INTRODUCTION

Since its establishment as a convenient tool for the study of magnetism and magnetic materials, the magneto-optical Kerr effect (MOKE) [1,2] has led to many relevant findings, such as the critical behavior in monolayers [3], the understanding of oscillatory interlayer exchange coupling [4], the spin reorientation transition [5], and the first detection of spin Hall states in semiconductors [6]. In recent years, MOKE has acquired further importance due to the emergence of novel research fields such as magnetoplasmonics [7,8] and the development of ultrafast lasers [9], which allow investigations on extremely short time scales [10,11], including all-optical magnetization reversal [12–14].

In nearly all MOKE studies, it is assumed for the sake of simplicity that the strength of the magneto-optical coupling factor Q, which defines the magnetization dependent elements in the dielectric tensor, is independent from the magnetization orientation, which essentially means that crystallographic structure and symmetry are not considered. Under this approximation, the dielectric tensor of a material exhibiting first-order magneto-optical Kerr effects is [2]

$$\overleftrightarrow{\varepsilon} = N^2 \begin{pmatrix} 1 & iQm_z & -iQm_y \\ -iQm_z & 1 & iQm_x \\ iQm_y & -iQm_x & 1 \end{pmatrix}, \qquad (1)$$

where m_x, m_y, and m_z are the normalized magnetization components along the x, y, and z axis, while the complex quantities N and Q are the refractive index and magneto-optical coupling factor of the material, respectively. It is evident from Eq. (1) that the off-diagonal elements of the dielectric tensor depend on the magnetization orientation, and it is this dependence from the individual magnetization components that leads to the well-known longitudinal, transverse, and polar Kerr effects [1,2]. However, a single complex factor Q is sufficient under this approximation to describe the coupling between the magnetization vector and the optical properties of the material. In the following, we refer to a material that possesses the dielectric tensor of Eq. (1) as a magneto-optically isotropic system, while we will refer to materials that cannot be described in this way as magneto-optically anisotropic systems.

The utilization of the dielectric tensor in Eq. (1) is generally understood to be a reasonable assumption for metallic systems, where optical anisotropies overall are weak [15], and very few experimental studies have observed only moderate deviations from this assumption [16–20]. However, all these prior works on magneto-optical anisotropy relied on different experimental geometries or even different samples in order to obtain Q values along different magnetization orientations. This has caused severe limitations for the accurate determination of magneto-optical anisotropy so far, and more importantly it has prohibited the investigation of magneto-optical anisotropy in conjunction with other materials properties, so that its underlying physical origin is unexplored [21]. It should also be mentioned that the accuracy and reliability of the widely utilized magneto-optical magnetometry could be diminished or even compromised if magneto-optical anisotropy effects were significant and not properly taken into account. Thus, this very popular methodology is actually reliant on the knowledge of magneto-optical anisotropy or the confirmation of its absence, both of which have been explored in very few individual cases only.

Here, we present our detailed study of magneto-optical anisotropy in epitaxial Co films of varying thickness. We observe magneto-optical anisotropy in all our films and we find a direct correlation between the amplitude of magneto-optical anisotropy and the magnitude of strain in our samples. In order to quantify the magneto-optical anisotropy in a precise and reliable way, we used generalized magneto-optical ellipsometry (GME) [22,23]. This technique's main advantage lies in its ability to simultaneously obtain optical and magneto-optical constants as well as magnetization orientation information with unprecedented precision. Furthermore, we take advantage of the vector magnetometry capability of GME to measure magnetic anisotropy, which in turn allows us to study the relation between magnetocrystalline anisotropy and magneto-optical anisotropy, which was also reported by the few earlier studies available on this subject [18–20]. In the following, we present the experimental aspects of our work in Sec. II, which includes the sample growth and measurement procedure. Then, our results are shown in Sec. III, where

*j.arregi@nanogune.eu

we demonstrate that magneto-optical anisotropy is increased by epitaxial strain. This observation is furthermore compared to the magnetocrystalline anisotropy features of our samples. Finally, we summarize the key aspects of our work and discuss their relevance in Sec. IV.

II. EXPERIMENTAL DETAILS

For our experimental study, we fabricated epitaxial hcp Co films with in-plane c axis orientation via sputter deposition onto hydrofluoric-acid-etched silicon substrates [24]. We followed the epitaxial sequence Si(110)/Ag(110)/Cr(211)/Co(10$\bar{1}$0), for which we deposited 75 nm of Ag and 50 nm of Cr as template layers and a sample-dependent thickness of Co. We also deposited 10 nm of amorphous SiO_2 on top of the Co films for oxidation protection. These particular samples are motivated by the fact that their magnetization reversal behavior is very simple given their uniaxial magnetocrystalline in-plane anisotropy. Correspondingly, quasistatic magnetization reversal occurs by means of magnetization rotation, followed by a sample-sized switch [25–27], so that an analysis of GME data sets in terms of uniform magnetization states is straightforward. Taking the specific nature of our samples and our experiment into account, the film magnetization will lie in the film plane throughout the entire reversal process. This is corroborated by our GME measurements, which determine the out-of-plane magnetization components to be less than 0.07% of the saturation magnetization in all cases. Thus, our analysis can be limited to in-plane magnetization orientations only [28].

Our magneto-optical characterization experiments utilize a setup that is schematically shown in Fig. 1(a). Light coming from a laser ($\lambda = 635$ nm) at 45º of incidence passes through a first rotatable Glan-Taylor polarizer (P1), is reflected by the sample, and finally detected by a photodiode after passing through a second rotatable polarizer (P2). The absolute orientation of the rotatable polarizers with respect to the plane of incidence is given by angles φ_1 and φ_2, and the sample is placed inside the gap of an electromagnet. The fractional intensity change upon magnetization reversal $\delta I/I = [I(H) - I(-H)]/(\frac{1}{2})[I(H) + I(-H)]$ that is measured by this type of setup is dependent on the reflection matrix $\tilde{R}$ of the sample and the polarizer orientations [22,23]. In order to reliably characterize $\tilde{R}$, measurements for different (φ_1, φ_2) configurations are carried out, building $\delta I/I(\varphi_1, \varphi_2)$ maps for each applied field value [23,28,29].

Experimental $\delta I/I(\varphi_1, \varphi_2)$ maps for the applied field strengths of 1700 Oe, 0 Oe and −300 Oe, are shown in Figs. 1(b)–1(d), respectively, for a 30 nm thick epitaxial Co film. Here, the GME sensitivity with respect to the magnetization orientation is well illustrated, which was facilitated by the fact that the sample was oriented at an angle of $\beta = 75^\circ$ between the applied field and the easy axis (EA) of magnetization. Longitudinal and transverse Kerr effects are superimposed in $\delta I/I$ maps and hence their pattern changes as the magnetization rotates upon sweeping the field [23,29]. For high fields [Fig. 1(b)] the longitudinal effect dominates, and the map shows two main lobes with opposite sign around the crossed polarizer configuration ($\varphi_1 = 90^\circ$, $\varphi_2 = 0^\circ$) [30]. As the field is decreased and then inverted [Figs. 1(c) and 1(d)] the

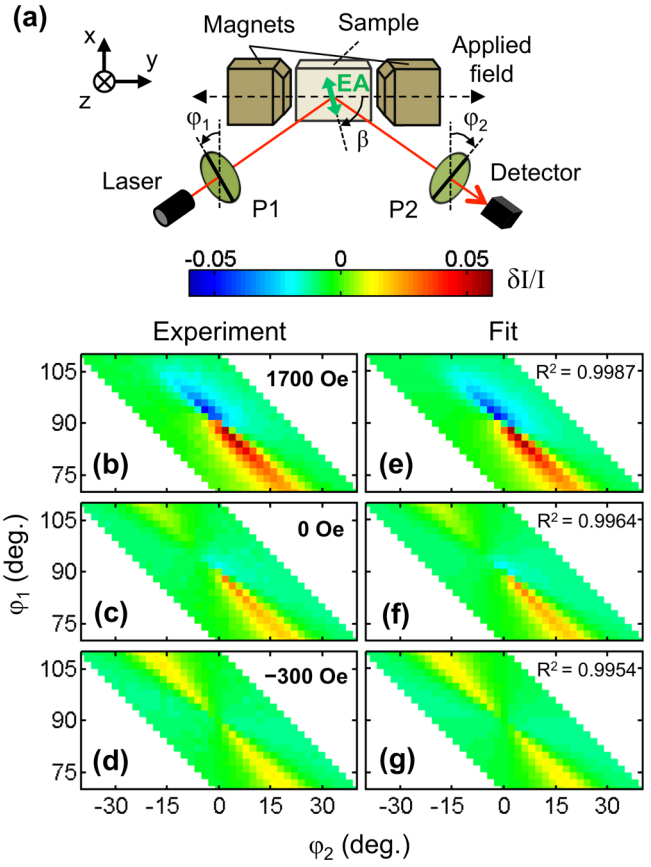

FIG. 1. (Color online) (a) Schematic of the GME setup. (b)–(d) Experimental $\delta I/I$ maps for a 30 nm thick epitaxial Co film at different applied field strengths H with the sample easy axis (EA) being oriented at $\beta = 75^\circ$. (e)–(g) Least-squares fits of $\delta I/I$ maps using the sample reflection matrix $\tilde{R}$ as fit parameter (R^2 goodness as indicated).

magnetization rotates, so that the transverse effect dominates causing the emergence of two positive lobes. All experimental $\delta I/I(\varphi_1, \varphi_2)$ maps were fitted with the elements of the optical reflection matrix $\tilde{R}$ as fit parameters, achieving excellent agreement with the experimental data. Exemplary fits are shown in Figs. 1(e)–1(g) side by side with the corresponding experimental maps. The goodness of the fit shows values better than $R^2 > 0.99$ in all cases.

III. RESULTS AND DISCUSSION

A. Magneto-optical anisotropy

To extract the dielectric tensor of our Co films, we used an appropriate optical model and applied the transfer matrix method [31–33] to calculate $\tilde{R}$ as a function of the optical model parameters. The optical model for our analysis is shown in the inset of Fig. 2(a). We use the measured refractive index of $n_0 = 1.46$ [34] for the SiO_2 cap layer and set $N_{Cr} = 3.13 + 3.31i$ for the Cr underlayer [35], which we consider to be the substrate in our optical model, because the light penetration depth at $\lambda = 635$ nm is significantly smaller than the combined thickness of the Co and Cr films. We first assume a conventional dielectric tensor for the Co

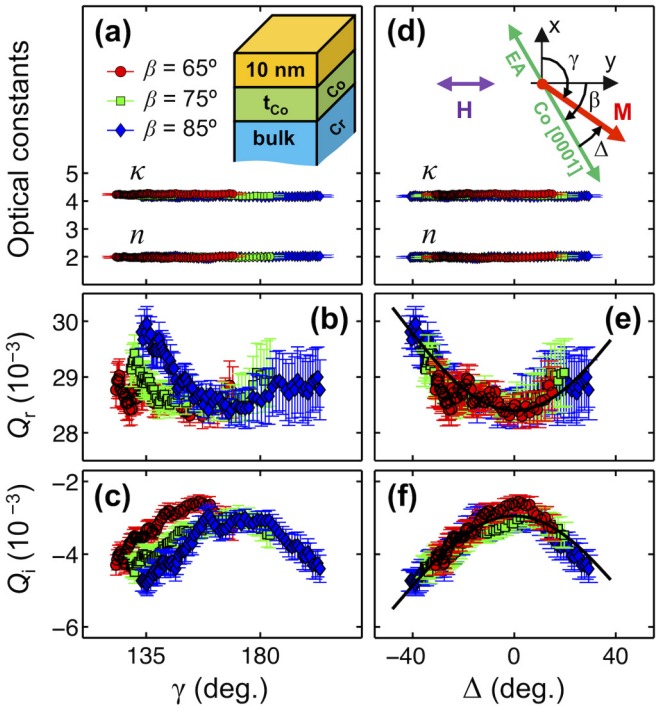

FIG. 2. (Color online) Optical model analysis for a 30 nm thick epitaxial Co film. (a) Optical constants n and κ, (b) Q_r, and (c) Q_i vs. the magnetization angle γ, for datasets with $\beta = 65°$, 75°, and 85°. The inset in (a) displays the multilayer structure of the optical model. (d) n and κ, (e) Q_r and (d) Q_i vs. the angle Δ. The inset in (d) defines the angles between the c axis of Co, the magnetization orientation, and the applied field. The solid lines in (e) and (f) represent the least-squares fits of the general dielectric tensor, Eq. (2), to the data.

film, in which Q is isotropic [Eq. (1)], in order to check for inconsistencies to occur in the presence of magneto-optical anisotropy. For every experimentally determined $\tilde{R}$, we obtain the best-matching model parameters for the optical ($N = n + i\kappa$) and magneto-optical ($Q = Q_r + iQ_i$) constants of the Co film and its magnetization orientation γ [see Fig. 2(d) inset] [36]. Results for the 30 nm thick Co film are shown in Figs. 2(a)–2(c) for $\beta = 65°$, 75°, and 85°. The data in this figure correspond to applied magnetic field values in the range from +2000 Oe to −400 Oe, for which the magnetization follows a field-dependent rotation at the angles β utilized here. While both n and κ [Fig. 2(a)] are magnetization orientation independent within our level of precision, the Q_r [Fig. 2(b)] and Q_i [Fig. 2(c)] values show a clear modulation with respect to the magnetization orientation γ, thus indicating the presence of magneto-optical anisotropy. However, the datasets for different β do not overlap and therefore indicate that γ, which is defined by the plane of incidence, is not a good variable to describe this anisotropy. Instead, a consistent description is achieved, if one uses the sample's crystallographic orientation as a reference frame. Figures 2(d)–2(f) show our experimental data vs. Δ, which is the magnetization angle with respect to the crystallographic c axis [see Fig. 2(d) inset]. While the trend of the optical constants is unaffected by this change in representation [Fig. 2(d)], the Q_r [Fig. 2(e)], and Q_i [Fig. 2(f)] vs. Δ data now exhibit a consistent behavior by collapsing onto the same line and showing symmetric behavior with respect to $\Delta = 0°$. This confirms that we observe here a magneto-optical anisotropy effect that is due to crystal symmetry.

In order to properly describe the observed behavior, we have to consider the following dielectric tensor for the Co film as defined in the crystal lattice reference frame

$$\overleftrightarrow{\varepsilon} = N^2 \begin{pmatrix} 1 & iQ_z\cos\psi & -iQ_\perp \sin\psi \sin\Delta \\ -iQ_z\cos\psi & 1 & iQ_\parallel \sin\psi\cos\Delta \\ iQ_\perp \sin\psi\sin\Delta & -iQ_\parallel \sin\psi\cos\Delta & 1 \end{pmatrix}, \quad (2)$$

which represents an optically isotropic material, but has the most general form to account for magneto-optical anisotropy [37]. In our experiment, the angle ψ between the z axis and the magnetization is 90°, while the in-plane angle Δ varies during the magnetization reversal. Hence, we access a two-dimensional projection of the dielectric tensor, while not measuring Q_z [38]. The quantities $Q_\parallel$ and $Q_\perp$ denote the magneto-optical coupling strength for magnetization orientations parallel and perpendicular to the crystallographic c axis within the surface plane. For in-plane magnetization orientations in our experimental geometry, one can derive from Eq. (2) that

$$Q(\Delta) = \frac{Q_\perp + Q_\parallel}{2}\left(1 - \frac{\tau}{2}\cos 2\Delta\right) \quad (3)$$

with $\tau = (Q_\perp - Q_\parallel)/[(Q_\perp + Q_\parallel)/2]$ being the fractional modulation amplitude of Q. We find our experimental data to be fully consistent with this crystal symmetry-induced Q anisotropy, as demonstrated by the overlap of the experimental data with the solid lines in Figs. 2(e) and 2(f), which are least-squares fit to the $Q(\Delta)$ functional form shown in Eq. (3) [39]. Specifically, the anisotropy amplitude for Q_r is 11.1%, and 88.1% for Q_i.

For the purpose of investigating the general relevance and the origin of magneto-optical anisotropy, we repeated this type of measurement and data analysis scheme for an entire series of epitaxial hcp Co samples with 5, 15, 50, 100, and 150 nm thicknesses. The good epitaxial quality of our samples in the entire thickness range is clearly demonstrated by Fig. 3(a), where θ–2θ scans for the different samples are shown. While the Ag and Cr peaks look virtually the same for all samples, the Co peak changes substantially in its relative intensity due to the varying sample thickness. X-ray diffraction measurements of the ω-scan peak width for Co(10$\underline{1}$0) and ϕ-scan peak width for Co(10$\underline{1}$1) do not show any substantial sample-to-sample variation, which corroborates that the crystalline quality for all our epitaxial Co films is independent from their thickness.

In all these Co films, we observe a magnetization orientation dependence of $Q = \tilde{Q}e^{i\vartheta} = Q_r + iQ_i$. Hereby, it is primarily the modulus $\tilde{Q}$ that varies strongly with the magnetization

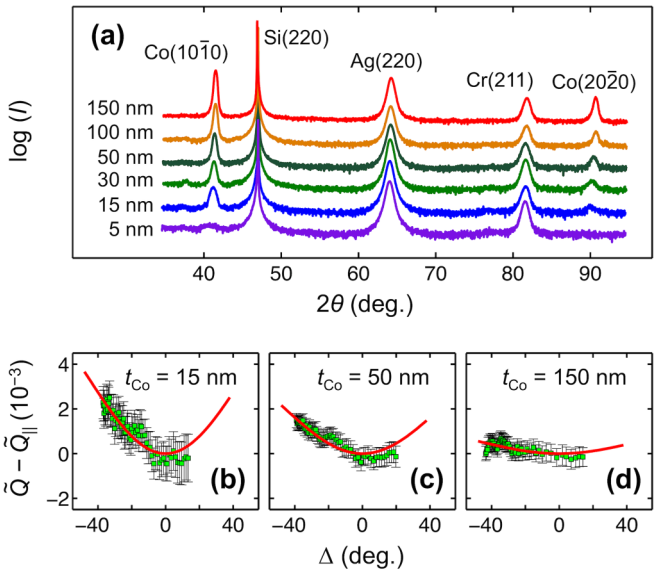

FIG. 3. (Color online) (a) $\theta-2\theta$ x-ray diffraction data for epitaxially grown Si(110)/Ag(110)/Cr(211)/Co(10$\bar{1}$0) samples of varying Co thickness; (b)–(d) magneto-optical coupling constant $\tilde{Q}$ vs. Δ for samples with (b) $t_{Co} = 15$ nm, (c) 50 nm, and (d) 150 nm. For all datasets, $\beta = 75^{\circ}$ was used. The solid lines show the least-squares fits of the general dielectric tensor, Eq. (2), to the data.

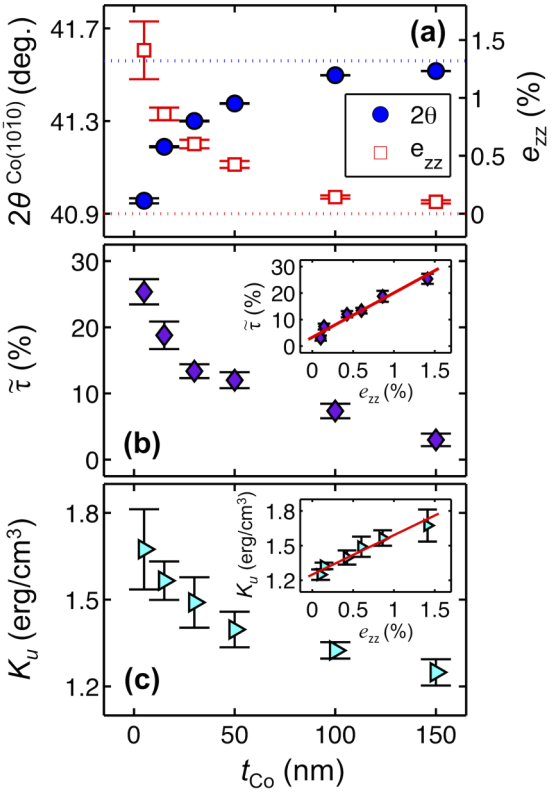

FIG. 4. (Color online) Thickness dependent Co film properties: (a) x-ray diffraction peak position (circles) and associated strain values e_{zz} (squares). The dotted lines indicate the bulk values. (b) Magneto-optical anisotropy amplitude $\tilde{\tau}$; the inset shows $\tilde{\tau}$ vs. e_{zz}. (c) Uniaxial magnetocrystalline anisotropy energy density K_u; the inset shows K_u vs. e_{zz}.

orientation, while the angle ϑ remains relatively constant. Figures 3(b)–3(d) display the magnetization orientation dependence of $\tilde{Q}$ for the 15 nm, 50 nm, and 150 nm thick Co films, respectively. The solid lines represent the best match to Eq. (3), from which we determine the modulation amplitudes of $\tilde{Q}$ to be 18.8%, 12.0%, and 2.9% for the 15 nm, 50 nm, and 150 nm thick Co films, respectively. Thus, we observe a very strong reduction of the magneto-optical anisotropy with increasing film thickness.

In order to understand this behavior, we have determined the level of strain in our epitaxial Co films. Fig. 4(a) displays how the Co(10$\bar{1}$0) peak position shifts towards higher values as the Co film thickness is increased. Furthermore, it is obvious that the peak position approaches $2\theta_{bulk} = 41.56^{\circ}$ for thicker films. Correspondingly, the out-of-plane strain $e_{zz} = (a - a_{bulk})/a_{bulk}$, with a being the hcp lattice constant in the basal plane, varies from positive 1.5% to nearly zero in our samples [Fig. 4(a)]. For comparison, Fig. 4(b) shows the thickness-dependent magneto-optical anisotropy amplitude $\tilde{\tau}$. It is evident that both quantities show very similar thickness-dependent behavior. The inset in Fig. 4(b) shows the direct comparison of $\tilde{\tau}$ with e_{zz}. The data display a clear correlation between both quantities, and thus provide evidence that the increase of magneto-optical anisotropy is directly connected to the epitaxial strain in our hcp Co films. The least-squares fit of these data to a straight line reveals a $\tilde{\tau}$ slope of 16.8 $\pm$ 1.4% for every 1% strain increase, as well as an estimated residual magneto-optical anisotropy amplitude of 3.3 $\pm$ 0.8% for the bulk case.

B. Magnetic anisotropy

Due to the fact that the main experimental as well as theoretical studies investigating magneto-optical anisotropy also emphasized its correlation with magnetocrystalline anisotropy [18–20,40,41], we have also studied this aspect here and compared both features with the structural properties of our samples. For this purpose, we have utilized the experimentally determined magnetization angle data $\Delta = \Delta(H, \beta)$ of our Co films and matched them to the free-energy expression

$$E = K_1 \sin^2\Delta + K_2 \sin^4\Delta - M_S H \cos(\Delta - \beta) \qquad (4)$$

utilizing a magnetocrystalline anisotropy energy expansion up to the fourth power term. Hereby, the magnetic anisotropy energy densities K_1 and K_2 are determined by treating them as fit parameters [42], which allows us to determine the total uniaxial magnetic anisotropy energy density $K_u = K_1 + K_2$. This quantity describes the energy difference between the magnetization being aligned along and perpendicular to the c axis of Co, corresponding to the minimum and maximum energy state in the absence of an applied magnetic field [43]. Figure 4(c) displays the thickness dependence of K_u, revealing a decline of about a 25% in its value upon increasing the film thickness as it changes from 1.67×10^6erg/cm^3 for the thinnest film to 1.25×10^6erg/cm^3 for the thickest one. Remarkably, the magnetic anisotropy energy shows a similar thickness-dependent decrease as the one we found for the magneto-optical anisotropy $\tilde{\tau}$, even if K_u does not approach

zero at high Co film thicknesses. Correspondingly, we observe a linear correlation also between K_u and e_{zz}, which is clearly visible in the inset of Fig. 4(c). A least-squares fit of these data to a straight line exhibits a slope of the magnetic anisotropy energy density of $(0.34 \pm 0.05) \times 10^6 \mathrm{erg/cm^3}$ per 1% increase in strain, as well as a zero-strain offset value of $(1.25 \pm 0.02) \times 10^6 \mathrm{erg/cm^3}$.

C. Strain-induced magneto-optical anisotropy and magnetic anisotropy

As shown above, we observe in our experiments on thin epitaxial Co films that the response to epitaxial strain for magneto-optical anisotropy and magnetocrystalline anisotropy is very similar. Indeed, it is well established that strain induces magnetocrystalline anisotropy by means of magnetoelastic coupling [44,45]. In the same way, theoretical reports on hcp Co explain the increase of the magnetocrystalline anisotropy energy upon the reduction of the crystallographic c/a ratio in terms of the strong correlation between this ratio and the splitting of the electronic d bands, which in turn lowers the band-filling factor [46,47].

While the connection between magnetocrystalline anisotropy and magneto-optical anisotropy has already been reported for Co films of different lattice symmetry, such as for fcc versus hcp Co [18,19], we demonstrate here that even small distortions of the crystal structure due to epitaxial strain can act as a most significant source of magneto-optical anisotropy. In prior studies of magneto-optical anisotropy for fcc Ni, it was suggested that its appearance was related to either second-order magneto-optical effects or magnetostriction [48]. We find these interpretations not to be applicable to our results. The GME methodology that we use removes any second-order magneto-optical effect from the data, so that the here observed magneto-optical anisotropy cannot be caused by them. Magnetostriction, on the other hand, should show a thickness dependence opposite to what we find here, since thicker epitaxial films can undergo larger shape changes than thinner ones due to the reduced relevance of the mechanical coupling to the substrate. In addition, it has also been suggested that magneto-optical anisotropy in bcc Fe can arise from third-order magneto-optical effects, given that the cubic crystal symmetry excludes the possibility of an anisotropic dielectric tensor for first-order magneto-optical effects [49]. While those effects could in principle be present in our experiment, there is no need to consider higher-order magneto-optical effects for hcp Co, as the hexagonal character of the crystal structure matches the specific symmetry that we found for the dielectric tensor. This fact is highlighted, for instance, in Figs. 2(e) and 2(f), where the consideration of an anisotropic dielectric tensor solely based on first-order magneto-optical effects proved to be sufficient to mimic the magnetization orientation dependence of the measured parameters. Moreover, we think that it is unlikely that third-order magneto-optical effects can add up to variations as large as the 25% of the total magneto-optical signal, given that it is well known that second-order effects are already one to two orders of magnitude weaker than first-order magneto-optical effects in hcp Co [50,51].

IV. CONCLUSIONS

In conclusion, we observe magneto-optical anisotropy in epitaxial Co films and find a direct correlation between the amplitude of this magneto-optical anisotropy and the film strain. Furthermore, our observations show very clearly that magneto-optical anisotropy effects are not generally small, even in only weakly strained metallic materials, for which the Q isotropy assumption is very widely utilized. Thus, relevant corrections to many past, present, and future MOKE experiments have to be contemplated. This is especially true for most common thin and ultrathin epitaxial films, for which strains that are far in excess of the 1.5% range explored here are typical. We also found that the magnetocrystalline anisotropy energy density exhibits a similar strain-dependent behavior if compared to the magneto-optical anisotropy, highlighting the fact that both effects are closely interrelated and originate from spin-orbit coupling, which is modified upon introducing lattice distortions in magnetic films. We observe this correlation between magneto-optical anisotropy and magnetocrystalline anisotropy, despite the fact that the magnetic anisotropy is an energy-integrated property involving all occupied electronic orbitals, while magneto-optical effects will arise only from certain electronic states that match the specific wavelength-dependent electronic transition condition [40,41]. Under these circumstances, we envision that the joint study of wavelength-dependent magneto-optical anisotropy and magnetic anisotropy experiments might provide a very relevant spectroscopic tool for the study of spin-orbit coupling effects in magnetic materials.

ACKNOWLEDGMENTS

We acknowledge funding from the Eusko Jaurlaritza (Program No. PI2012-47) and the Ministerio de Economía y Competitividad (Spain) (Project No. MAT2012-36844). J.A.A. acknowledges Ministerio de Economía y Competitividad (Spain) for support from Grant No. BES-2010-035194. O.I. acknowledges the Eusko Jaurlaritza for support from Grant No. BFI09.284.

[1] M. J. Freiser, IEEE Trans. Magn. **4**, 152 (1968)
[2] Z. Q. Qiu and S. D. Bader, J. Magn. Magn. Mater. **200**, 664 (1999)
[3] C. Liu and S. D. Bader, J. Appl. Phys. **67**, 5758 (1990)
[4] Z. Q. Qiu, J. Pearson, A. Berger, and S. D. Bader, Phys. Rev. Lett. **68**, 1398 (1992)
[5] D. Li, M. Freitag, J. Pearson, Z. Q. Qiu, and S. D. Bader, Phys. Rev. Lett. **72**, 3112 (1994)
[6] Y. K. Kato, R. C. Myers, A. C. Gossard, and D. D. Awschalom, Science **306**, 1910 (2004)
[7] B. Sepúlveda, J. B. González-Díaz, A. García-Martín, L. M. Lechuga, and G. Armelles, Phys. Rev. Lett. **104**, 147401 (2010)

[8] N. Maccaferri, A. Berger, S. Bonetti, V. Bonanni, M. Kataja, Q.H. Qin, S. van Dijken, Z. Pirzadeh, A. Dmitriev, J. Nogues, J. Åkerman, and P. Vavassori, Phys. Rev. Lett. **111**, 167401 (2013)

[9] U. Keller, Nature (London) **424**, 831 (2003)

[10] B. Koopmans, M. van Kampen, J. T. Kohlhepp, and W. J. M. de Jonge, Phys. Rev. Lett. **85**, 844 (2000)

[11] M. Cinchetti, M. Sánchez Albaneda, D. Hoffmann, T. Roth, J.-P. Wüstenberg, M. Krauß, O. Andreyev, H. C. Schneider, M. Bauer, and M. Aeschlimann, Phys. Rev. Lett. **97**, 177201 (2006)

[12] A. V. Kimel, A. Kirilyuk, P. A. Usachev, R. V. Pisarev, A. M. Balbashov, and Th. Rasing, Nature (London) **435**, 655 (2005)

[13] C. D. Stanciu, F. Hansteen, A. V. Kimel, A. Kirilyuk, A. Tsukamoto, A. Itoh, and Th. Rasing, Phys. Rev. Lett. **99**, 047601 (2007)

[14] C.-H. Lambert, S. Mangin, B. S. D. Ch. S. Varaprasad, Y. K. Takahashi, M. Hehn, M. Cinchetti, G. Malinowski, K. Hono, Y. Fainman, M. Aeschlimann, and E. E. Fullerton, Science **345**, 1337 (2015).

[15] Th. Herrmann, K. Lüdge, W. Richter, K. G. Georgarakis, P. Poulopoulos, R. Nünthel, J. Lindner, M. Wahl, and N. Esser, Phys. Rev. B **73**, 134408 (2006)

[16] G. S. Krinchik, E. A. Ganshina, and V. S. Gushchin, J. Physique **32**, C1-1061 (1971)

[17] E. A. Ganshina, G. S. Krinchik, L. S. Mironova, and A. S. Tablin, Sov. Phys. JETP **51**, 369 (1980).

[18] D. Weller, G. R. Harp, R. F. C. Farrow, A. Cebollada, and J. Sticht, Phys. Rev. Lett. **72**, 2097 (1994)

[19] R. M. Osgood, III, K. T. Riggs, A. E. Johnson, J. E. Mattson, C. H. Sowers, and S. D. Bader, Phys. Rev. B **56**, 2627 (1997)

[20] L. Uba, S. Uba, V. N. Antonov, A. N. Yaresko, T. Ślęzak, and J. Korecki, Phys. Rev. B **62**, 13731 (2000)

[21] A recent work [D. Schmidt, C. Briley, E. Schubert, and M. Schubert, Appl. Phys. Lett. **102**, 123109 (2013)] reports on magneto-optical anisotropy for permalloy films with slanted columnar topography. However, the authors did not separate magnetization orientation effects from Q anisotropy, so that magneto-optical anisotropy in our sense here was not actually measured.

[22] A. Berger and M. R. Pufall, Appl. Phys. Lett. **71**, 965 (1997)

[23] A. Berger and M. R. Pufall, J. Appl. Phys. **85**, 4583 (1999)

[24] W. Yang, D. N. Lambeth, and D. E. Laughlin, J. Appl. Phys. **85**, 4723 (1999)

[25] O. Idigoras, P. Vavassori, J.M. Porro, and A. Berger, J. Magn. Magn. Mat. **322**, L57 (2010)

[26] O. Idigoras, A. K. Suszka, P. Vavassori, P. Landeros, J. M. Porro, and A. Berger, Phys. Rev. B **84**, 132403 (2011)

[27] O. Idigoras, A. K. Suszka, P. Vavassori, B. Obry, B. Hillebrands, P. Landeros, and A. Berger, J. Appl. Phys. **115**, 083912 (2015)

[28] J. A. Arregi, J. B. González-Díaz, E. Bergaretxe, O. Idigoras, T. Unsal, and A. Berger, J. Appl. Phys. **111**, 103912 (2012)

[29] J. A. Arregi, J. B. González-Díaz, N. Soriano, B. Mora, and A. Berger, J. Phys. D: Appl. Phys. **48**, 305002 (2015)

[30] In order to check our experimental results, we performed measurements in the vicinity of another crossed polarizer configuration ($\varphi_1 = 0^\circ$, $\varphi_2 = 90^\circ$), in addition to the configuration shown in the manuscript ($\varphi_1 = 90^\circ$, $\varphi_2 = 0^\circ$), finding that both results are consistent with each other.

[31] Š. Višňovský, Czech. J. Phys. B **36**, 625 (1986)

[32] J. Zak, E. R. Moog, C. Liu, and S. D. Bader, Phys. Rev. B **43**, 6423 (1991)

[33] M. Schubert, Phys. Rev. B **53**, 4265 (1996)

[34] We have previously shown that oxide capping layers can introduce optical anisotropy in epitaxial systems [J. B. González-Díaz, J. A. Arregi, E. Bergaretxe, M. J. Fertin, O. Idigoras, and A. Berger, J. Magn. Magn. Mater. **325**, 147 (2013)]. We have corrected for this fact in our optical model, even though it does not impact the strength of the magneto-optical anisotropy we report here.

[35] P. B. Johnson and R. W. Christy, Phys. Rev. B **9**, 5056 (1974)

[36] The robustness of the dielectric tensor fit is independent on the initial conditions for n, κ, Q_r and Q_i, achieving a rapid convergence upon the utilization of bulk hcp Co values. However, the correct half-space for the initial guess of the magnetization angle γ needs to be assumed, since the off-diagonal elements of the dielectric tensor are bilinear in Q and the magnetization components [Eq. (1)]. Thus, one can only separate the corresponding sign of these parameters by taking into account the field-cycle history for the initial value of γ.

[37] Š. Višňovský, Czech. J. Phys. B **36**, 1424 (1986)

[38] Due to the crystal structure of hcp Co we expect Q_z and $Q_\perp$ to be identical, at least in the limit of weakly strained systems, because both describe magneto-optical coupling for basal plane orientations of the magnetization.

[39] It is not possible to determine the anisotropic Q and the magnetization angle from an individual $\delta I/I$ map. Instead, the magnetization angles γ and Δ retrieved from individual $\delta I/I$ map fits have to be corrected by using the magneto-optically anisotropic dielectric tensor of Eq. (2), a fact that is already implemented for the data shown in Fig 2.

[40] G. Y. Guo and H. Ebert, Phys. Rev. B **50**, 10377 (1994)

[41] P. M. Oppeneer, T. Kraft, and H. Eschrig, Phys. Rev. B **52**, 3577 (1995)

[42] For in-plane magnetization reversal events, it is not possible to have access to the absolute values of K_1 and K_2 by fitting the magnetization angle data to the energy expression in Eq. (4). Thus, only the quantities K_1/M_S and K_2/M_S can be accessed. Correspondingly, the values of M_S for all samples have been determined by vibrating sample magnetometry. Their values ranged between 1350 and 1400 emu/cm^3 for the entire sample series.

[43] W. Yang, D. N. Lambeth, and D. E. Laughlin, J. Appl. Phys. **87**, 6884 (2000)

[44] D. Sander, Rep. Prog. Phys. **62**, 809 (1999)

[45] D. Sander, J. Phys. Condens. Matter **16**, R603 (2004)

[46] G. H. O. Daalderop, P. J. Kelly, and M. F. H. Schuurmans, Phys. Rev. B **41**, 11919 (1990)

[47] A. Sakuma, J. Phys. Soc. Jap. **63**, 3053 (1994)

[48] M. R. Parker, Phys. Stat. Sol. B **49**, 299 (1972)

[49] A. V. Petukhov, Th. Rasing, T. Katayama, N. Nakajima, and Y. Suzuki, J. Appl. Phys. **83**, 6742 (1998)

[50] R. M. Osgood, III, B. M. Clemens, and R. L. White, Phys. Rev. B **55**, 8990 (1997)

[51] R. M. Osgood, III, S. D. Bader, B. M. Clemens, R. L. White, and H. Matsuyama, J. Magn. Magn. Mater. **182**, 297 (1998)